RSC Advances

PAPER

View Article Online
View Journal | View Issue

Cite this: *RSC Adv.*, 2026, **16**, 19620

Deprotonation- and TICT-triggered ultra-large Stokes shift of aqueous NIR-emissive hydroxylstryryl-pyridinium derivatives

Xiaolong Lu,[abc] Liyu Xiong,[bc] Zhihan Zhang,[bc] Haolong Yang,[bc] Enmin Li *[def] and Hefeng Zhang *[bc]

Received 17th March 2026
Accepted 8th April 2026

DOI: 10.1039/d6ra02237e

rsc.li/rsc-advances

Hydroxystyryl-pyridinium derivatives serving as fluorescent dyes with water-soluble conjugated skeletons exhibited remarkably large Stokes shifts of up to 404 nm and tunable deep-red to near-infrared (NIR) emissions, which are attributed to the enhanced charge transferring triggered by excited-state deprotonation of the phenol group and twist intramolecular charge transfer.

Organic fluorescent materials hold considerable promise across diverse fields such as chemical biosensing, optoelectronic devices, and bioimaging.[1–6] Among them, a large Stokes shifts is critically helpful for fluorescent dyes as it effectively minimizes self-absorption and background interference, thereby significantly enhancing the signal-to-noise ratio and detection sensitivity in applications such as high-contrast bioimaging and anti-counterfeiting.[5–8] However, the widespread adoption of conventional fluorescent dyes including established families like rhodamine,[9,10] BODIPY,[11–13] and cyanine[14–17] are limited by their small Stokes shift, typically less than 50 nm. The narrow gap between excitation and emission wavelengths leads to severe self-absorption and re-excitation, causing signal cross-talk and compromising the sensitivity and accuracy of detection and anti-counterfeiting technologies.[18–21] Furthermore, issues such as low luminescence efficiency in aggregate states and poor solubility in aqueous environments significantly restrict their practical utility in biological and environmental settings.[13,17,22–25]

To address the limitations of small Stokes shifts, several molecular design strategies have been explored. A prominent approach involves the construction of donor–acceptor (D–A) or donor–π–acceptor (D–π–A) systems, where intramolecular charge transfer (ICT) can create a significant difference in electron cloud distribution and dipole moment between the excited and ground states and thus cause moderate increase in the Stokes shift.[5,26–30] Moreover, the construction of the D–π–A structure is one of the most powerful and widely used strategy to extend emission wavelengths. More sophisticated mechanisms to enhance Stokes shift, primarily including excited-state intramolecular proton transfer (ESIPT),[31–38] which induces a substantial energy loss *via* rapid proton transfer after excitation, and the formation of a twisted intramolecular charge transfer (TICT)[38–44] state in donor–π–acceptor systems, where significant structural reorganization leads to a large Stokes shift. Besides, ICT and ESIPT mechanisms can effectively increase the Stokes shift and have been tremendously important for the development of fluorescence chemical sensors and imaging probes,[29–33] the TICT mechanism plays a core role in fields such as aggregation-induced emission (AIE),[38] crystallization-induced emission enhancement (CIEE),[39] and metal–organic frameworks (MOFs),[45] owing to its combination of significant molecular conformational reorganization and charge transfer characteristics. As an example, Peng[40] *et al.* reported a viscosity-responsive endoplasmic reticulum targeting NIR fluorescent probe HBT-PP based on the twisted intramolecular charge transfer (TICT) and the excited state intramolecular proton transfer (ESIPT), which exhibited a Stokes shift up to 320 nm. In addition, to manipulate a single emitter unit, incorporating two fluorophores with short and length emission wavelength, respectively, into fluorescence resonance energy transfer (FRET) cassettes or designing specific molecular skeletons can also achieve a large "pseudo"-Stokes shift determined by the energy difference between the donor's absorption

[a]*Marine Science Institute, College of Science, Shantou University, Shantou 515063, China*

[b]*Key Laboratory for Preparation and Application of Ordered Structural Materials of Guangdong Province, Department of Chemistry, College of Chemistry and Chemical Engineering, Shantou University, Shantou 515063, China. E-mail: hfzhang@stu.edu.cn*

[c]*GuangDong Engineering Technology Research Center of Advanced Polymer Synthesis, College of Chemistry and Chemical Engineering, Shantou University, Shantou 515063, China*

[d]*The Key Laboratory of Molecular Biology for High Cancer Incidence Coastal Chaoshan Area, Department of Biochemistry and Molecular Biology, Shantou University Medical College, Shantou 515041, Guangdong, China. E-mail: nmli@stu.edu.cn*

[e]*The Laboratory for Cancer Molecular Biology, Shantou Academy Medical Sciences, Shantou 515041, China*

[f]*Chaoshan Branch of State Key Laboratory for Esophageal Cancer Prevention and Treatment, Shantou 515063, China*

and the acceptor's emission.[45–47] Cui[45] *et al.* incorporated the photoisomerizable molecule spiropyran as an energy transfer intermediate, and two fluorescent dyes coumarin 153 (Cou153) and methylene blue (MB) within a metal–organic frameworks (MOFs), which achieving the dual-color dynamic luminescent material with NIR fluorescence at 700 nm and a maximum Stokes shift of 300 nm.

Beyond molecular engineering, strategies operating at the aggregate level, such as forming J-aggregates and incorporating aggregation-induced emission (AIE) moieties, provide effective pathways to amplify the Stokes shift. J-aggregation significantly enhances the Stokes shift primarily through two interconnected mechanisms, the distinctive "head-to-tail" slip-stacked molecular packing and the subsequent facilitation of excited-state structural relaxation and intermolecular charge transfer. Furthermore, J-aggregated state can restrict intramolecular motions that typically dissipate energy non-radiatively in single molecules, thereby channeling more energy into excited-state geometric relaxation, which further enlarges the energy difference between absorption and emission.[48–50] Similarly, introduction of aggregation-induced emission (AIE) groups like tetraphenylethene can significantly enhance the Stokes shift by restricting intramolecular motion (RIM).[34,37,42,43] However, active intramolecular rotations/vibrations of AIEgenic moieties in solution provide dominant non-radiative decay pathways, resulting in weak emission and a convoluted Stokes shift. In addition, molecular encapsulation strategies, such as the incorporation of fluorescent molecules within metal–organic frameworks (MOFs) or cyclodextrins, can effectively enhance the Stokes shift of the fluorophores by constraining intramolecular motion and promoting excited-state proton transfer processes.[45,50,51] Despite sustained efforts, achieving exceptionally large Stokes shifts greater than 400 nm in organic fluorophores, especially in small molecules and UV-visible region, remains a significant challenge, underscoring the need for novel design strategies.

Inspired by our recent reported deprotonation-caused red-shifting of emission in hydroxystyryl-pyridinium (SP-OH) dyes, herein, a series of SP-OH derivatives were developed, and an ultra-large Stokes shift up to 404 nm were discovered.

The SP-OH dyes were synthesized *via* a Knoevenagel condensation catalysed by ammonium acetate (Scheme 1). As an example, the SP-2-NO_2-5-OH was prepared by coupling commercially available 5-hydroxy-2-nitrobenzaldehyde with pre-synthesized 1-(2-hydroxyethyl)-4-methylpyridinium bromide. The same synthetic strategy was applied to afford the full library of SP-X-Py derivatives. All intermediates and final products were fully characterized by ^{1}H and ^{13}C nuclear magnetic resonance (NMR) spectroscopy and high-resolution mass spectrometry (HRMS) (see Experimental section in SI, Fig. S13–S26). In the SP-OH dyes skeleton, the phenol group serves as an electron-donor (D), the nitro group attaching onto the phenyl and the vinyl-bridged pyridinium behave as electron-acceptors (A). The conjugated D–π–A skeleton promised long-wavelength emission due to the intramolecular charge-transfer.

All the SP-OH dyes showed significant absorptions and fluorescent emissions in various organic solvents ($c = 10^{-5}$ M). The full UV-Vis absorption spectra of all derivatives in different solvents are presented in Fig. S1, which reveals the broad absorption characteristics of SP-OH dyes in the UV to visible range; corresponding fluorescence emission spectra are shown in Fig. S2. The pH-dependent UV-Vis absorption and fluorescence emission spectra of SP-OH dyes in aqueous solution are shown in Fig. S3 and S4, which directly reflect the deprotonation behavior of phenolic hydroxyl group under different pH conditions (Fig. 1, S1, S2, Tables 1 and S1–S4). The absorption and fluorescence emission spectra of SP-OH dyes were first investigated in dimethylformamide (DMF) solutions ($c = 10^{-5}$ M) (Fig. 1). All derivatives exhibited broad absorption bands in the UV to visible range and red emissions with large Stokes shifts (Table 1). Practically, SP-2-NO_2-5-OH-Py showed main absorption at 304 nm, with two side peaks at 331 nm and 422 nm, and the emission at 600 nm with a large Stokes shift up to 296 nm and QY of 6.6%. In contrast, the SP-5-NO_2-2-OH-Py also showed 3 absorption peaks, but with the main peak at 513 nm, and red-shifted emission at 642 nm with QY of 9.2%, indicating significant influence of positional effect on their absorption and emission behaviours. To further disclose the role of phenolic hydroxyl group, SP-2-NO_2-Py and SP-2-NO_2-5-OMe-Py were designed as the blank control in which the hydroxyl group was eliminated and etherified, respectively. SP-2-NO_2-Py absorbed at 351 nm and an emission peak at 591 nm, resulting in a Stokes shift of 240 nm. SP-2-NO_2-5-OMe-Py

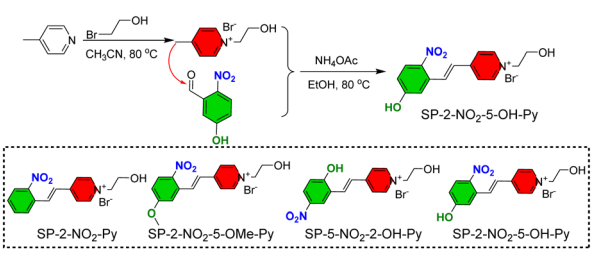

Scheme 1 Easy synthesis of SP-OH derivatives through Knoevenagel condensation reaction.

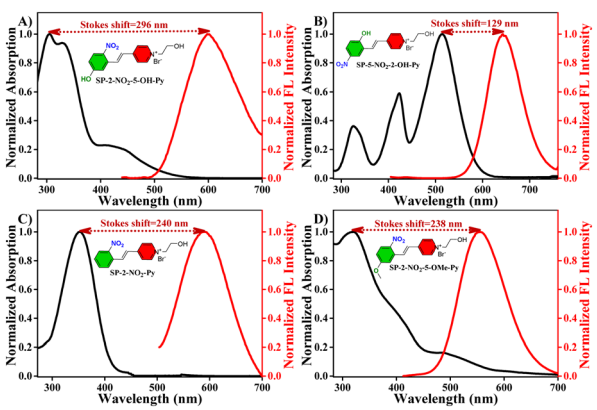

Fig. 1 Normalized absorption and fluorescent emission spectra in DMF ($c = 10^{-5}$ M). Green: donor (D); red: acceptor (A).

Table 1 Photophysical characteristics of SP-OH dyes

Sample[a]	λ_{abs}/nm	λ_{ex}/nm	λ_{em}/nm	Stokes shift/nm	ε $\times 10^4$/M^{-1} cm^{-1}	QY/%
SP-2-NO_2-5-OH-Py	304	360	600	296	5.86	6.6
SP-5-NO_2-2-OH-Py	513	385	642	129	3.04	9.2
SP-2-NO_2-Py	351	410	591	240	4.08	2.6
SP-2-NO_2-5-OMe-Py	317	393	555	238	5.64	14.7

[a] Absorptions, fluorescent emission, molar extinction coefficients (ε) and absolute photoluminescence quantum yields (QY) (integrating sphere method) were measured in DMF solution ($c = 10^{-5}$ M).

showed broad absorption at 317 nm and emitted at 555 nm, with a shift of 238 nm. The molar extinction coefficients (ε) ranged from 4.08 to 5.86 $\times$ 10^4 M^{-1} cm^{-1}, indicating strong light-absorbing ability, while the absolute fluorescence quantum yields (QY) varied from 2.6% to 14.7%. The low QYs are attributed to non-radiative decay pathways such as molecular vibrations or rotation.

To disclose effect of potential deprotonation of the phenolic hydroxyl group, the absorption and emission of SP-OH dyes were investigated in solvents of varying polarity, including chloroform ($CHCl_3$), dichloromethane (DCM), acetonitrile (MeCN), DMF and DMSO, *etc.* (Fig. 2). In contrast to SP-5-NO_2-2-OH-Py which exhibited absorption at longest wavelength among the dyes, the SP-2-NO_2-5-OH-Py showed unexpected absorption at shortest wavelength (<310 nm). Interestingly, both SP-5-NO_2-2-OH-Py and SP-2-NO_2-5-OH-Py exhibited longer emission wavelengths than that of their analogues without hydroxyl group. The increase of solvent polarity caused red shifting of the emission. For example, emission wavelength SP-2-NO_2-5-OH-Py extended from 585 nm to 610 nm. The short-wavelength absorption and long-wavelength emission promised large Stokes shift.

The fluorescence performance in aqueous media is particularly important for biological applications. In water, the SP-OH dyes maintained large Stokes shifts, as detailed in Fig. 3 and Table 2. Especially, SP-2-NO_2-5-OH-Py showed absorption at 305 nm (UV region) and NIR emission at 709 nm and an ultra-large Stokes shift of up to 404 nm is achieved which is one of the largest reported for organic fluorophores. Besides, after 180 min of continuous light irradiation, SP-2-NO_2-5-OH-Py can still maintain 40% of its fluorescence intensity, indicating that it has good photostability (Fig. S5). SP-5-NO_2-2-OH-Py exhibited two absorption peaks at 319 nm and 366 nm, respectively. And it showed red emission at 608 nm and large Stokes shifts of 289 nm and 242 nm. In contrast, SP-2-NO_2-Py showed a smaller shift of 155 nm (absorption at 313 nm, emission at 468 nm), emphasizing the critical effect of phenolic hydroxyl group, which further proved the results showed by SP-2-NO_2-5-OMe-Py with Stokes shift of 234 nm. The molar extinction coefficients in water remained high (*e.g.*, 7.06 $\times$ 10^4 M^{-1} cm^{-1} for SP-2-NO_2-5-OH-Py), but quantum yields decreased to 0.8–4.4% due to strong interaction between dyes and water molecules.

Due to the determinative effect of pH over the deprotonation of phenolic hydroxyl group, the fluorescence behaviors of SP-OHs were investigated in aqueous solutions with varying pH (Fig. 4, S3, S4 and Tables S5–S8). In alkali solutions, deprotonation of phenol group and electrostatic interaction between quaternary ammonium moiety and hydroxide coexist, which enhance and suppress electron transferring across the D–π–A conjugated skeleton of SP-OH, respectively. It is believed that in SP-OH containing a phenolic hydroxyl group, the proton-transfer pathway dominates and thus lead to the long-wavelength emissions.

In case of SP-2-NO_2-5-OH-Py and SP-5-NO_2-2-OH-Py, due to pH-dependent protonation, both two dyes showed absorption at ~411 nm and 441 nm at high pH, which significantly blue-shifted to the UV region at ~305 nm and 350 nm at low pHs.

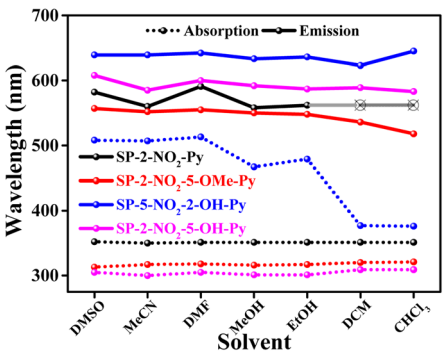

Fig. 2 The solvent-dependent absorption and emission wavelength of SP-OH dyes ($c = 10^{-5}$ M).

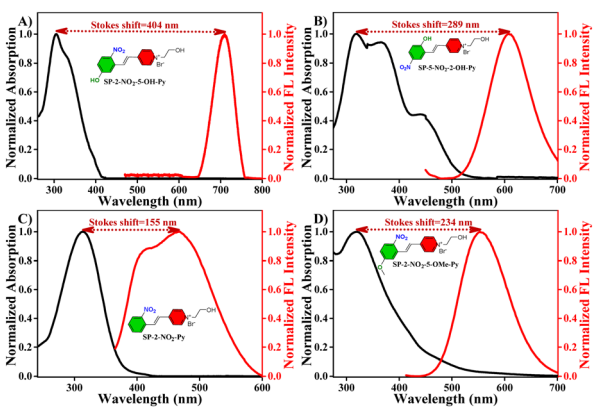

Fig. 3 Normalized absorption and fluorescent emission spectra in water ($c = 10^{-5}$ M). Green: donor (D); red: acceptor (A).

Table 2 Photophysical characteristics of SP-OH dyes

Sample[a]	λ_{abs}/nm	λ_{ex}/nm	λ_{em}/nm	Stokes shift/nm	$\varepsilon \times 10^4/M^{-1}$ cm^{-1}	QY/%
SP-2-NO_2-5-OH-Py	305	450	709	404	7.06	1.9
SP-5-NO_2-2-OH-Py	319/366	380	608	289/242	2.70/2.53	4.4
SP-2-NO_2-Py	313	345	468	155	3.09	0.8
SP-2-NO_2-5-OMe-Py	319	393	553	234	8.29	4.3

[a] Absorptions, fluorescent emission, molar extinction coefficients (ε) and absolute photoluminescence quantum yields (QY) (integrating sphere method) were measured in aqueous solution ($c = 10^{-5}$ M).

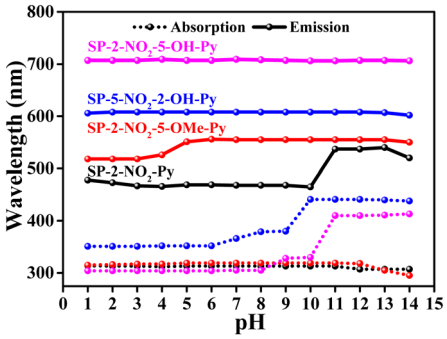

Fig. 4 pH-dependent absorption and emission wavelength of SP-OH dyes ($c = 10^{-5}$ M in water).

The long-wavelength absorption at high pH is attributed to the neutralization of acidic phenolic hydroxyl group. The deprotonation generated a negatived charge which further greatly prompted charge transfer induced by the positive-charged pyridinium group. In contrast, after elimination of hydroxyl group, the resulting dyes of SP-2-NO_2-5-OMe-Py and SP-2-NO_2-Py as control showed slightly red-shift with the pH decreasing, which is caused by the weaken charge transfer by the large amount of OH^- with strong negative charge (Scheme 2). Surprisingly, the emission of both of SP-2-NO_2-5-OMe-Py and SP-2-NO_2-5-OH-Py are not effected by the pH, which clearly indicated a consist structure at S_1 state, suggesting a deprotonation process at excited state.

Upon photoexcitation, the deprotonation and twisted intramolecular charge transfer (TICT) process of the SP-2-NO_2-5-OH-Py molecule form a synergistic effect of mutual promotion, ultimately leading to an ultra-large Stokes shift of 404 nm.

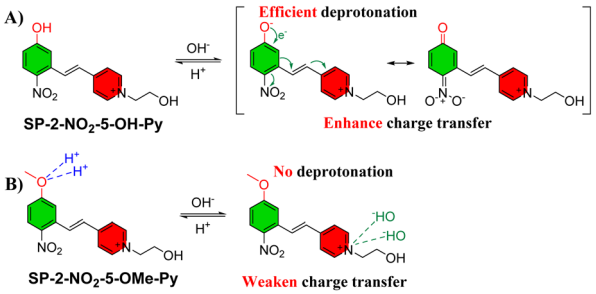

Scheme 2 Comparison of pH on charge transferring of (A) SP-2-NO_2-5-OH-Py and (B) SP-2-NO_2-5-OMe-Py.

To prove the mechanism for the ultra-large Stokes shifts of SP-OH dyes, especially SP-2-NO_2-5-OH-Py, density functional theory (DFT) and time-dependent density functional theory (TD-DFT) calculations were performed at B3LYP/6-311+G(d,p) level[52] (Fig. S7–S10). As shown in Fig. 5 and S11, all the SP-OH dyes have significantly distorted dihedral angle between the phenol and pyridinium rings (75.2–83.6°) in the excited state (S_1). The large twisted structure endows the SP-OH dyes with the characteristic of exhibiting significant fluorescence emission under solid-state conditions (Fig. S6). In ground state (S_0), in contrast to SP-5-NO_2-2-OH-Py showing planar structure, due to the large steric hindrance effect of the nitro group, dihedral angles were observed in all SP-2-NO_2-5-OH-Py (45.8°), SP-2-NO_2-5-OMe-Py (37.7°), and SP-2-NO_2-Py (35.5°). The highest occupied molecular orbital (HOMO) localized on the electron donor in both S_0 and S_1 states, whereas the lowest unoccupied molecular orbital (LUMO) on electron acceptor. The twisted intramolecular charge transfer (TICT) effect caused large Stokes shift of all the nitro-contained dyes.

In addition to comparison of dihedral angle, the changes of bond length of SP-OH dyes before and after excitation were investigated. Taking SP-2-NO_2-5-OH-Py and SP-5-NO_2-2-OH-Py as an example, after excitation, the bond length of O–H in phenol group increases from 0.964 Å to 0.970 Å and from 0.965 Å to 0.970 Å (Fig. 6). The deprotonation in excited state leads to increasing of the electron density on oxygen atom and thus enhancement of charge transferring to the pyridinium moiety, which promises these molecules red-shifted emission and a large Stokes.

Based on the above analysis, the dual synergistic effect of the TICT and the deprotonation effect enable SP-2-NO_2-5-OH-Py to have the largest Stokes shift (>400 nm).

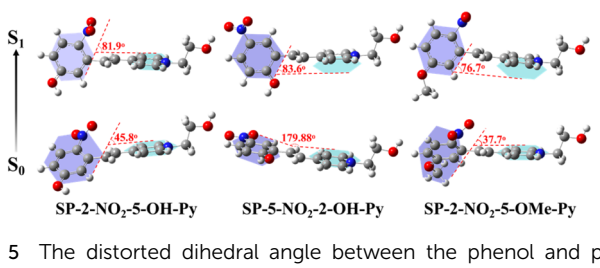

Fig. 5 The distorted dihedral angle between the phenol and pyridinium rings of SP-OH dyes in the ground state (S_0) and the excited state (S_1).

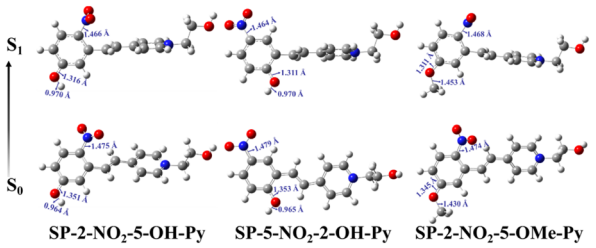

Fig. 6 The bond length of SP-OH dyes in the ground state (S_0) and the excited state (S_1).

Conventional invisible fluorescent inks are typically limited to blue emission. Developing long-wavelength versions is challenging because they must remain invisible under daylight, which requires negligible absorption in the visible range. The SP-OH-Py dyes overcome this limitation due to their exceptionally large Stokes shift. This enables the preparation of an invisible ink that shows no color in daylight but emits bright orange fluorescence under UV excitation. This distinct optical signature is difficult to replicate with existing technologies, thereby significantly enhancing anti-counterfeiting security (Fig. S12).

In summary, a series of hydroxystyryl-pyridinium derivatives were facilely synthesized. These dyes show remarkable optical properties in aqueous solution, among which SP-2-NO_2-5-OH-Py exhibits an ultra-large Stokes shift up to 404 nm with UV absorption and NIR emission. Mechanistic studies reveal that the large Stokes shift arises from the synergistic effect of excited-state deprotonation and twisted intramolecular charge transfer (TICT). Benefiting from their unique optical features, these dyes can be used as invisible anti-counterfeiting inks with high security. This work provides a new strategy for constructing large Stokes shift fluorophores and offers promising candidates for bioimaging, sensing, and anti-counterfeiting applications.

Conflicts of interest

There are no conflicts to declare.

Data availability

The data supporting this article have been included as part of the supplementary information (SI). Supplementary information: materials, experimental details, data details, computational details, NMR spectra, and optical images of anti-counterfeiting. See DOI: https://doi.org/10.1039/d6ra02237e.

Acknowledgements

This work was supported by the National Natural Science Foundation of China (82273108) and Guangdong provincial Scientific and Technological Innovation Program (STKJ2023073, 2024A1515012747).

References

1 J. W. Zhang, K. C. Zhang, K. Wang, B. Wang, S. Y. Zhu, H. P. Qian, Y. M. Ma, M. L. Zhang, T. Y. Liu, P. Chen, Y. Shen, Y. Z. Fu, S. L. Fang, X. X. Zhang, P. Zou, W. L. Deng, Y. Ma and Z. X. Chen, *Nat. Methods*, 2025, **22**, 1276–1287.
2 R. J. Ming, Z. X. Xue, Y. L. Xu, Z. H. Zhang, Z. X. Chen, J. S. Miao and C. L. Yang, *Angew. Chem., Int. Ed.*, 2025, **64**, e202516696.
3 J. Y. Wang, H. R. Zheng, X. W. Xiao and X. F. Luo, *Chem. Commun.*, 2025, **61**, 7434–7437.
4 Q. N. Liu, Z. Y. Li, Y. J. Huang, Z. N. Lin, X. C. Shen and H. Chen, *Chem. Sci.*, 2025, **16**, 23394–23404.
5 S. Y. Wu, Z. C. Ban, H. Tang, N. Ma, X. Y. Ran, Q. Zhou, Y. H. Zhang, Z. Y. Wang and X. Q. Yu, *Chem. Commun.*, 2025, **61**, 10574–10577.
6 S. A. H. Ahmed, X. Gao, Y. Zheng, H. T. Wang, S. Zeng, H. Liu and L. H. Qian, *Anal. Chim. Acta*, 2025, **1367**, 344299.
7 R. P. Bhatta, S. Sumit, V. Kachwal, V. Vishwakarma, A. R. Choudhury and I. R. Laskar, *J. Mater. Chem. C*, 2024, **12**, 12906–12918.
8 P. Lu, M. D. Zhou, Y. J. Yuan, Y. Yan and H. L. Zhang, *Adv. Opt. Mater.*, 2024, **12**, 2400359.
9 J. M. Ritz, A. Khakimzhan, J. J. Dalluge, V. Noireaux and E. M. Puchner, *J. Am. Chem. Soc.*, 2025, **147**, 7588–7596.
10 Z. J. Luo, K. R. Bhuskute, Y. X. Cao, J. Tang and A. Kaur, *Angew. Chem., Int. Ed.*, 2026, e19056.
11 J. Y. Zhao, L. Q. Ren, D. R. Lan, B. Q. Zhan, J. Y. Zhang, J. Mu and C. He, *Nat. Commun.*, 2025, **16**, 9719.
12 F. Lv, X. Guo, S. S. Zhu, S. Huang, L. Li, S. Z. Wang, L. J. Jiao and E. H. Hao, *Chem. Commun.*, 2025, **61**, 4975–4978.
13 C. Schad, C. Ray, C. Diaz Norambuena, S. Serrano-Buitrago, F. Moreno, B. L. Maroto, I. Garcia-Moreno, M. Munoz-Ubeda, I. Lopez-Montero, J. Banuelos and S. D. L. Moya, *Chem. Sci.*, 2025, **16**, 8030–8039.
14 W. Z. Ding, M. Jia, S. K. Yao, Z. P. Liu, F. W. Xu, M. F. Li, C. Q. Wang, W. J. He, Y. C. Chen and Z. J. Guo, *J. Am. Chem. Soc.*, 2025, **147**, 47835–47847.
15 H. Q. Huang, Y. N. Wu, X. He, Y. H. Liu, J. H. Zhu, M. R. Gu, D. H. Zhou, S. R. Long, Y. H. Chen, L. Wang, M. L. Li, X. Q. Chen and X. J. Peng, *Adv. Sci.*, 2025, **12**, 2416905.
16 Y. K. Yue, J. H. Ai, W. J. Chi, X. N. Zhao, F. J. Huo and C. X. Yin, *Adv. Mater.*, 2024, **36**, 2408450.
17 Z. P. She, R. Li, F. Zeng and S. Z. Wu, *Adv. Healthcare Mater.*, 2024, **13**, 2400791.
18 Y. Yuan, S. Z. Xiong, L. Q. Lv, W. Hu, X. X. Xiong, C. Y. Li and H. P. Deng, *Chem. Eng. J.*, 2023, **471**, 144341.
19 P. Chowdhury, Z. Y. Lu, S. P. Su, M. H. Liu, C. Y. Lin, M. W. Wang, Y. C. Luo, Y. J. Lee and H. K. Chiang, *Adv. Healthcare Mater.*, 2024, **13**, 2400606.
20 X. W. Li, J. H. Ai, Y. R. Zhang, F. J. Huo and C. X. Yin, *Nano Today*, 2025, **63**, 102768.
21 Z. P. Chen, L. Yang, W. J. Xu, F. F. Xu, J. R. Sheng, Q. Xiao, X. Z. Song and W. Q. Chen, *Anal. Chem.*, 2023, **95**, 3325–3331.

22 F. L. Ma, Q. Jia, Z. W Deng, B. Z. Wang, S. W. Zhang, J. H. Jiang, G. C. Xing, Z. L. Wang, Z. J. Qiu, Z. Zhao and B. Z. Tang, *ACS Nano*, 2024, **18**, 9431–9442.
23 W. L. Tan, Y. Yu, T. Y. Shi, L. T. Zhang, H. L. Gan, B. H. Wang, G. L. Liu, M. K. Li, L. Yang and Y. G. Ma, *Adv. Mater.*, 2024, **36**, 2410418.
24 R. M. Jiang, Z. S. Liu, Y. Y. Han, J. W. Long, T. Gao, X. Lan, M. G. Yu, T. Fang, H. J. Ma, Y. Wei, B. Z. Tang and Z. J. Zhao, *Chem. Eng. J.*, 2024, **500**, 157575.
25 M. L. Wang, X. Q. Wang, D. J. Xu, C. J. Yu and Y. P. Wang, *Chem. Commun.*, 2026, **62**, 915–918.
26 Y. X. Sun, Y. F. Lin, Q. Zhou, Y. X. Han, M. J. Mao, L. H. Guo, H. Y. Liu and J. B. Wang, *Sens. Actuators, B*, 2025, **444**, 138527.
27 H. Y. Zheng, W. K. Peng, M. M. Liu, M. Li, W. W. Li, J. Y. Xing, P. F. Shi, Q. Wang, S. S. Zhang and L. Yang, *Anal. Chem.*, 2025, **97**, 2472–2478.
28 J. Gao, F. Li, J. Chen, Y. K. Gao, C. F. Fan, Y. Huang, H. F. Yu, X. T. Yang and X. C. Wang, *Sens. Actuators, B*, 2024, **398**, 134696.
29 A. Pal, M. Karmakar, S. R. Bhatta and A. Thakur, *Coord. Chem. Rev.*, 2021, **448**, 214167.
30 C. S. Abeywickrama, *Chem. Commun.*, 2022, **58**, 9855–9869.
31 A. C. Sedgwick, L. L. Wu, H. H. Han, S. D. Bull, X. P. He, T. D. James, J. L. Sessler, B. Z. Tang, H. Tian and J. Yoon, *Chem. Soc. Rev.*, 2018, **47**, 8842–8880.
32 Y. H. Li, D. Dahal, C. S. Abeywickrama and Y. Pang, *ACS Omega*, 2021, **6**, 6547–6553.
33 H. Gu, W. J. Wang, W. Y. Wu, M. L. Wang, Y. R. Liu, Y. J. Jiao, F. Wang, F. Wang and X. Q. Chen, *Chem. Commun.*, 2023, **59**, 2056–2071.
34 M. Liu, B. Feng, F. Y. Chu, D. Y. Fan, F. Zhang, F. Chen and W. B. Zeng, *Chin. Chem. Lett.*, 2025, **36**, 110043.
35 J. K. Wang, C. H. Wang, C. C. Wu, K. H. Chang, C. H. Wang, Y. H. Liu, C. T. Chen and P. T. Chou, *J. Am. Chem. Soc.*, 2024, **146**, 3125–3135.
36 S. Z. Yi, B. N. Li, P. Y. Fu, M. Pan and C. Y. Su, *ACS Appl. Mater. Interfaces*, 2023, **15**, 3172–3181.
37 Z. Hu, J. L. Li, L. L. Feng, Y. L. Zhu, R. X. Zhao, C. H. Yu, R. C. Xu, W. Z. Wang, H. Ding and P. P. Yang, *Nano Lett.*, 2024, **24**, 16426–16435.
38 M. M. Islam, Z. Hu, Q. S. Wang, C. Redshaw and X. Feng, *Mater. Chem. Front.*, 2019, **3**, 762–781.
39 H. Naito, K. Nishino, Y. Morisaki, K. Tanaka and Y. Chujo, *Angew. Chem., Int. Ed.*, 2017, **56**, 254–259.
40 Z. Liu, C. Y. Zhang, Z. P. Li, W. Y. Ma, J. Liu, X. Xia, N. Xu, W. Sun, J. J. Du, J. L. Fan and X. J. Peng, *Sci. China: Chem.*, 2025, **68**, 360–368.
41 X. J. Yan, R. C. Feng, J. J. Fu, Q. Q. Han, Y. L. Liu and Q. Song, *Angew. Chem., Int. Ed.*, 2025, **64**, e202516458.
42 L. Zhao, H. Zhu, Y. Y. Duo, D. W. Pang, Z. G. Wang and S. L. Liu, *Adv. Healthcare Mater.*, 2023, **12**, 2301584.
43 M. Ojha, M. Banerjee, M. Mandal, T. Singha, S. Ray, P. K. Datta, M. Mandal, A. Anoop and N. D. P. Singh, *ACS Appl. Mater. Interfaces*, 2024, **16**, 21486–21497.
44 C. Wang, W. C. Jiang, D. Tan, L. Huang, J. Li, Q. L. Qiao, P. Yadav, X. G. Liu and Z. C. Xu, *Chem. Sci.*, 2023, **14**, 4786–4795.
45 C. Y. Li, H. Q. Zheng, W. L. Xu, Z. Y. Xu, Z. L. Liao, G. D. Qian and Y. J. Cui, *Adv. Mater.*, 2025, **10**, e18371.
46 X. L. Zhou, L. Miao, W. Zhou, Q. L. Qiao and Z. C. Xu, *Chin. Chem. Lett.*, 2025, **36**, 110984.
47 C. J. Yin, Z. A. Yan, R. J. Yan, C. Xu, B. B. Ding, Y. H. Ji and X. Ma, *Adv. Funct. Mater.*, 2024, **34**, 2316008.
48 K. W. Lee, Y. J. Gao, W. C. Wei, J. H. Tan, Y. P. Wang, Z. Feng, Y. H. Zhang, Y. Liu, X. L. Zheng, C. Cao, H. Chen, P. F. Wang, S. L. Li, K. T. Wong and C. S. Lee, *Adv. Mater.*, 2023, **35**, 2211632.
49 N. Zhang, L. Liu, H. X. Chang, K. Liu, T. H. Liu, L. P. Ding and Y. Fang, *J. Phys. Chem. Lett.*, 2023, **14**, 7283–7289.
50 M. Orfano, J. Perego, C. X. Bezuidenhout, I. Villa, R. Lorenzi, B. Sabot, S. Pierre, S. Bracco, S. Piva, A. Comotti and A. Monguzzi, *Adv. Funct. Mater.*, 2024, **34**, 2404480.
51 M. X. Qin, W. L. Ji, P. C. Huang, F. Y. Wu and L. Q. Mao, *Anal. Chem.*, 2024, **96**, 14697–14705.
52 T. Lu and F. W. Chen, *J. Comput. Chem.*, 2012, **33**, 580–592; T. Lu, *J. Chem. Phys.*, 2024, **161**, 082503.